Contribution from the Department of Chemistry and Chemical Engineering and the Saskatchewan Accelerator Laboratory, University of Saskatchewan, Saskatoon, Saskatchewan S7N 0W0, Canada, and the Hahn-Meitner-Institut für Kernforschung Berlin GmbH, Bereich Strahlenchemie, D-1000 Berlin 39, Federal Republic of Germany

Formation and Characterization of Platinum(III)–Ammonia Complex Ions Using Pulse Radiolysis

HASAN M. KHAN,[1a] WILLIAM L. WALTZ,*[1a] JOCHEN LILIE,[1b] and ROBERT J. WOODS[1a]

Received June 10, 1981

The reactions of hydroxyl radical with tetraammineplatinum(II) perchlorate and of the hydrated electron with *trans*-dihydroxotetraammineplatinum(IV) perchlorate have been investigated in aqueous media with the fast-reaction technique of pulse radiolysis in conjunction with conductivity and UV–visible absorption detection. The kinetic studies have been supplemented by final-product analysis on pulse-irradiated solutions for the formation of free ammonia and for changes in the concentration of platinum(II). The hydroxyl radical reaction proceeds by an addition process to the platinum(II) center, with a rate constant of $(6.6 \pm 0.4) \times 10^9$ M^{-1} s^{-1}. The hydrated electron reduces the platinum(IV) complex with a rate constant of $(4.9 \pm 0.3) \times 10^{10}$ M^{-1} s^{-1}. The nascent products of these reactions are transitory species in which the metal has a formal oxidation state of III, and evidence is presented to support their formulation as $Pt(NH_3)_4(H_2O)(OH)^{2+}$ and $Pt(NH_3)_4(OH)_2^+$, respectively. Both species exhibit intense absorption bands with peaks near 270 nm, and they undergo reactions to yield three further transients, one of these being $Pt(NH_3)_4(H_2O)_2^{3+}$ absorbing in the region of 250 nm. The two additional transients, arising at a secondary level, exhibit absorption bands of lesser intensity with peaks in the region of 340 and 530 nm. The nature of these species and their long-term reactions are discussed. A mechanism is proposed whereby the foregoing intermediates are interrelated by acid–base, ammonia substitution, and water elimination processes.

Introduction

There has been within recent years an increasing number of reports concerning the occurrence of platinum coordination compounds and organometallic complexes in which the metal center is formally in the unusual oxidation state of III.[2-22] This activity has been engendered in part by the recognition that Pt(III) complexes can play an important mechanistic role as intermediates in a variety of different chemical contexts. These are generally associated with one-electron equivalent processes drawn from the areas of electrochemistry, photochemistry, thermal noncomplementary oxidation–reduction processes, or radiation chemistry. Attention has also been directed to the possible involvement of Pt(III) and Pt(I) ammine intermediates as sensitizing agents associated with the potential use of platinum compounds in combination with radiation therapy.[23,24] Owing to the fact that Pt(III) complexes are generally of a transitory existence, their presence in a number of circumstances has been inferred indirectly from observed rate laws and overall reaction stoichiometries. The use of the fast-reaction technique of pulse radiolysis (and to a lesser extent flash photolysis) affords however a highly advantageous means to generate and characterize platinum(III) systems in a direct fashion. The applicability of this approach has been demonstrated through the investigations of platinum(III) complex ions containing halogen and pseudohalogen ligands as well as ones incorporating bi- and tridentate amine and amino acid chelates. Notwithstanding the significance of these studies, the interpretations of the results have been restricted owing to the frequent occurrence of more than one transient and the limitations imposed by the general reliance on one detection technique, namely, UV–visible absorption spectroscopy.

In this report, which focuses on platinum(III) ammonia complex ions, we have endeavored to enlarge the scope of such investigations by the use of several detection techniques: the investigation of different routes for the generation of the transients and analysis for some of the final products formed on *pulse irradiation*. Specifically, the reactions of hydroxyl radical with tetraammineplatinum(II) ion and of the hydrated electron with *trans*-dihydroxotetraammineplatinum(IV) ion have provided alternative pathways to the generation of common intermediates. Of note with regard to the electron reaction has been the detection and characterization of the nascent product $Pt(NH_3)_4(OH)_2^+$. The identification of this intermediate has provided in part the basis for a more detailed development of the type of reaction mechanism recently reported for the corresponding platinum(III)–ethylenediamine complexes.[20] (In the latter case, the analogous electron product was not observed directly.) Both conductivity and absorption detection techniques have been employed in this work. The former has proven particularly useful in elucidating the

(1) (a) University of Saskatchewan. (b) Hahn-Meitner-Institut.
(2) Adams, G. E.; Broszkiewicz, R. K.; Michael, B. D. *Trans. Faraday Soc.* **1968**, *64*, 1256.
(3) Belluco, U. "Organometallic and Coordination Chemistry of Platinum"; Academic Press: New York, 1974; pp 166–170.
(4) Brodovitch, J. C.; Storer, D. K.; Waltz, W. L.; Eager, R. L. *Int. J. Radiat. Phys. Chem.* **1976**, *8*, 465.
(5) Broszkiewicz, R. K.; Grodkowski, J. *Int. J. Radiat. Phys. Chem.* **1976**, *8*, 359.
(6) Buxton, G. V.; Sellers, R. M. *Coord. Chem. Rev.* **1977**, *22*, 195.
(7) Chen, J. Y.; Kochi, J. K. *J. Am. Chem. Soc.* **1977**, *99*, 1450.
(8) Glennon, C. S.; Hand, T. D.; Sykes, A. G. *J. Chem. Soc., Dalton Trans.* **1980**, 19.
(9) Ghosh-Mozumdar, A. S.; Hart, E. J. *Int. J. Radiat. Phys. Chem.* **1969**, *1*, 165.
(10) Hall, J. R.; Plowman, R. A. *Aust. J. Chem.* **1955**, *8*, 158.
(11) Halpern, J.; Pribanić, M. *J. Am. Chem. Soc.* **1968**, *90*, 5941.
(12) Loginov, A. V.; Shagisultanova, G. A. *Zh. Prikl. Khim. (Leningrad)* **1976**, *49*, 2353.
(13) Loginov, A. V.; Yakoulev, V. A.; Shagisultanova, G. A. *Koord. Khim.* **1979**, *5*, 733.
(14) (a) Miller, J. S.; Epstein, A. J. *Prog. Inorg. Chem.* **1976**, *20*, 1. (b) Eisenberg, R. *Ibid.* **1970**, *12*, 295. (c) McCleverty, J. A. *Ibid.* **1968**, *10*, 49.
(15) Peloso, A. *J. Chem. Soc., Dalton Trans.* **1979**, 1160.
(16) Sen Gupta, K. K.; Sen, P. K.; Sen Gupta, S. *Inorg. Chem.* **1977**, *16*, 1396.
(17) Stasicka, Z.; Marchaj, A. *Coord. Chem. Rev.* **1977**, *23*, 131.
(18) Storer, D. K.; Waltz, W. L.; Brodovitch, J. C.; Eager, R. L. *Int. J. Radiat. Phys. Chem.* **1975**, *7*, 693.
(19) Summa, G. M.; Scott, B. A. *Inorg. Chem.* **1980**, *19*, 1079.
(20) Waltz, W. L.; Lilie, J.; Walters, R. T.; Woods, R. J. *Inorg. Chem.* **1980**, *19*, 3284.
(21) Waltz, W. L.; Woods, R. J.; Whitburn, K. D. *Photochem. Photobiol.* **1978**, *28*, 681.
(22) Waltz, W. L.; Brodovitch, J. C.; Kundu, K. P. *Radiat. Phys. Chem.* **1977**, *10*, 77.
(23) Douple, E. B.; Richmond, R. C. In "Cisplatin: Current Status and New Developments"; Prestakeys, A., Crooke, S. T., Carter, S. K., Eds.; Academic Press: New York, 1980; Chapter 8.
(24) Richmond, R. C.; Simic, M. G. *Br. J. Cancer, Suppl.* **1978**, *No. 3*, 20.

0020-1669/82/1321-1489$01.25/0

acid–base and ligand substitution properties of the platinum(III) complex ions. The kinetic results obtained by these means and in conjunction with final-product analysis for free ammonia have allowed for reasonable assignments to be made as to the natures of the intermediates and have provided further support for earlier proposals that such species can exhibit different structures.[2,4,9,20,22] Previous reports on related systems have also suggested on the basis of kinetic results that the ultimate disappearance of Pt(III) intermediates proceeds by disproportionation reactions to yield Pt(II) and Pt(IV) products. Our determinations for the overall concentration changes of Pt(II), coupled with kinetic observations, allude to a more complicated behavior.

Experimental Section

Materials and Solutions. Tetraammineplatinum(II) perchlorate was prepared from the chloride salt, obtained commercially (Platinum Chemicals, Alfa Division of Ventron Corp., K and K Labs Division of ICN Pharmaceuticals Inc.).[25] Samples of the perchlorate compound were characterized by comparison of the near-UV absorption spectrum, recorded on a Cary 118C spectrophotometer, with that reported[26] and by elemental analysis. Anal. Calcd for $[Pt(NH_3)_4](ClO_4)_2$: Pt, 42.2; N, 12.12. Found (typical analysis): Pt, 42.0; N, 12.17. *trans*-Dihydroxotetraammineplatinum(IV) perchlorate was prepared as follows. $[Pt(NH_3)_4](ClO_4)_2$ (1.04 g) was dissolved in 30 mL of an aqueous solution containing 10 mL of 30% H_2O_2 and 0.03 mL of concentrated $HClO_4$. The solution was heated at 70 °C until the volume was reduced to 15 mL. On subsequent cooling in an ice bath, a white precipitate formed, which was collected, recrystallized from a minimum amount of aqueous $NaClO_4$, and then dried under vacuum (yield ca. 95%). Anal. Calcd for $[Pt(NH_3)_4(OH)_2](ClO_4)_2$: Pt, 39.3; Cl, 14.29; N, 11.29. Found: Pt, 38.8; Cl, 14.29; N, 11.28. The UV spectrum exhibited a general increase in absorption from 350 to 210 nm without discernible peaks, in agreement with previous results.[27,28]

All solutions used for pulse-radiolysis experiments, carried out at about 23 °C, were prepared just prior to use with triply distilled water or water purified by a Millipore Super-Q system. Such solutions were deaerated by procedures which are described elsewhere[20] and which made use of argon, helium, or nitrous oxide gases. The pH of the solutions was adjusted by addition of reagent grade $HClO_4$ or NaOH and was measured by pH meter, calibrated with certified buffer solutions. All other materials were of reagent grade.

Product Analysis. Pulse-irradiated solutions were analyzed for released ammonia and for changes in total Pt(II) content by the following spectrophotometric methods. The determination of ammonia was based upon its reaction with hypochlorite and phenol to give indophenol with an absorption maximum at 625 nm in basic media.[29] This analysis can be employed to detect ammonia concentrations as low as about 1 μM (1-cm cell); however, the color development is sensitive to a number of parameters (volume and order of addition of reagents, temperature, and pH). The following procedure lead to reproducible results. To a 50-mL volumetric flask were added with shaking freshly prepared reagents in the order: 10 mL of test solution, 20 mL of saturated boric acid solution, 5 mL of Cl_2 saturated water, and 5 mL of 8% phenol solution. The mixture was heated in a water bath at 80 °C for 3 min and cooled in an ice bath and then 5 mL of 3 M NaOH was added. The solution (diluted to mark) was placed in a water bath (25 °C) for 15 min before the absorbance was measured at 625 nm. The test solutions comprised the pulse-irradiated and unpulsed platinum solutions to which known amounts of ammonia (as NH_4Cl or NH_4ClO_4) were added after irradiation. The slopes and intercepts for the linear plots of absorbance vs. the concentration of added ammonia were determined by least-square regression analysis. The slopes for the irradiated and unirradiated solutions were compared by use of a "t" test (95% confidence limit) in order to discern if the values were statistically different. If they were not, an average slope value was used along with the difference in the intercept values to calculate the concentration of ammonia released by pulse irradiation.

Analysis for changes in the total Pt(II) concentration upon irradiation made use of the oxidation of Pt(II) to Pt(IV) by $K_2[IrCl_6]$ in 0.2 M HCl and 0.2 M NaCl solutions (25 °C).[11] The oxidant, $IrCl_6^{2-}$, exhibits a strong absorption peak at 487 nm (ϵ 4020 ± 40 M^{-1} cm^{-1}) whereas other species present do not absorb significantly at this wavelength. So that the procedure could be calibrated, varying amounts of $Pt(NH_3)_4^{2+}$ (50–250 μM) were added to solutions containing 550 μM $IrCl_6^{2-}$ on an equal volume basis. The results indicated that the decrease in absorbance was linear with Pt(II) concentration and that the stoichiometric ratio was 2:1 $IrCl_6^{2-}$:Pt(II). The results were not sensitive to the initial pH of the test solutions (pH 5.0–10.0) nor to the presence of the following agents, which were or could be present in irradiated solutions: acetone (0.4 M), *tert*-butyl alcohol (0.2 M), H_2O_2 (50–400 μM), isopropyl alcohol (2.0 M), *trans*-$Pt(NH_3)_4(OH)_2^{2+}$ (50–100 μm), *trans*-$Pt(NH_3)_4(Cl)_2^{2+}$ (40–60 μM). In the absence of Pt(IV), 70 μM of hydrazine had no effect; however, in the presence of 60 μM $Pt(NH_3)_4Cl_2^{2+}$, it gave a positive test for Pt(II). Owing to the low concentrations of other Pt(II) complex ions which might be formed under irradiation conditions, it was not feasible to identify their specific compositions although such possible products are likely to be aquated species such as *cis*-$Pt(NH_3)_2(H_2O)_2^{2+}$. Performance of this test on a solution containing 123 μM *cis*-$Pt(NH_3)_2(H_2O)_2^{2+}$ indicated that oxidation by $IrCl_6^{2-}$ was quantitative. Our experience with this complex and $Pt(NH_3)_4^{2+}$ and that of others[11,13] with related Pt(II) complexes would suggest that the results obtained by the foregoing procedure provided a valid measure of the total concentration of Pt(II) present. Generally three to seven successive pulses were performed in order to form sufficient amounts of product material for analysis, and no dependency on the number of pulses was found.

Pulse-Radiolysis Apparatus and Dosimetry. The apparatus employing conductivity and optical detection techniques and associated dosimetry have been described elsewhere.[20] Of note is that the transient signals represent differences between that of the unirradiated and the pulsed solutions. Such differences were calibrated against one of the following dosimetry solutions: $Fe(CN)_6^{4-}$, thiocyanate, or tetranitromethane. The absorption spectra were recorded on a point-to-point basis, generally at 10-nm intervals, with an optical cell of 3.93-cm light path. The *G* values (number of a given species formed per 100 eV of energy absorbed) and the equivalent ionic conductivities for the species of interest to this work are given elsewhere.[20] The errors cited with respect to the values of the rate constants are the estimates of the standard deviations.

Results

Primary Reactions of Aqueous Free Radicals with Platinum Complexes. Pulse irradiation of dilute aqueous solutions by high-energy electrons (2–20 MeV in this study) leads to the generation of aqueous free radicals, hydrogen ion, and smaller amounts of H_2 and H_2O_2.

$$H_2O \xrightarrow{e^-} e_{aq}^-, H, OH, H^+, H_2, H_2O_2 \qquad (1)$$

So that possible complications arising from the presence initially of several radical species could be minimized, standard scavenging procedures were employed.[30–33] In the study of the reaction of OH and $Pt(NH_3)_4^{2+}$, the solutions were saturated with nitrous oxide: N_2O reacts with e_{aq}^- to yield OH.[30] While hydrogen atom also reacts with $Pt(NH_3)_4^{2+}$, our studies of this reaction indicate that this process was of minor concern under the conditions of this work.[34] The reaction of OH and

(25) Mason, W. R.; Johnson, R. C. *Inorg. Chem.* **1965**, *4*, 1258.
(26) Mason, W. R.; Gray, H. B. *J. Am. Chem. Soc.* **1968**, *90*, 5721.
(27) Johnson, R. C.; Widner, C. G. *Inorg. Chem.* **1979**, *18*, 2027.
(28) The spectrum recorded here for *trans*-$[Pt(NH_3)_4(OH)_2](ClO_4)_2$ corresponds closely to that found by R. C. Johnson (personal communication): this work, ϵ 2.15 × 10^3 M^{-1} cm^{-1} (220 nm); that reported for *trans*-$[Pt(NH_3)_4(OH)_2]SO_4$, 2.0 × 10^3 M^{-1} cm^{-1} (220 nm).[27]
(29) Bolleter, W. T.; Bushman, C. J.; Tidwell, P. W. *Anal. Chem.* **1961**, *33*, 592.
(30) Anbar, M.; Bambenek, M.; Ross, A. B. *Natl. Stand. Ref. Data Ser. (U.S., Natl. Bur. Stand.)* **1973**, *NSRDS–NBS43*.
(31) Dorfman, L. M.; Adams, G. E. *Natl. Stand. Ref. Data Ser. (U.S., Natl. Bur. Stand.)* **1973**, *NSRDS–NBS46*.
(32) Anbar, M.; Farhataziz; Ross, A. B. *Natl. Stand. Ref. Data Ser. (U.S., Natl. Bur. Stand.)* **1975**, *NSRDS–NBS51*.
(33) Simic, M.; Neta, P.; Hayon, E. *J. Phys. Chem.* **1969**, *73*, 3794.
(34) Khan, H. M.; Waltz, W. L.; Woods, R. J.; Lilie, J. *Can. J. Chem.*, in press.

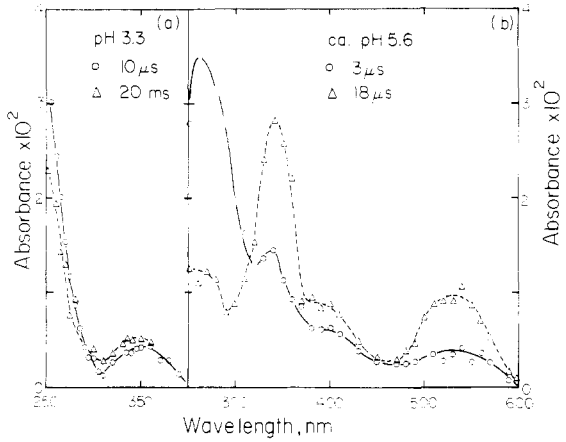

Figure 1. Absorption spectra arising from the reaction of OH and $Pt(NH_3)_4^{2+}$ in solutions saturated with N_2O: (a) pH 3.3, 200 μM $Pt(NH_3)_4^{2+}$, ca. 6.9 μM OH at 10 μs (O) and at 20 ms (Δ); (b) natural pH of ca. 5.6, 80 μM $Pt(NH_3)_4^{2+}$, ca. 3.4 μM OH at 3 μs (O) and at 18 μs (Δ).

$Pt(NH_3)_4^{2+}$ was investigated at a pH of about 5.6 (natural pH) by monitoring the growth in absorption at 315 nm, an isosbestic point in the absorption spectrum for the resulting products. With concentrations of $Pt(NH_3)_4^{2+}$ (18–62 μM) considerably in excess of that for OH, the change in absorption obeyed a first-order rate law. A plot of the observed rate constant, k_{obsd}, vs. complex concentration was linear. The second-order rate constant of $(6.6 \pm 0.4) \times 10^9$ M^{-1} s^{-1} was calculated from the slope of the plot.

The rate constant for the reaction of e_{aq}^- and *trans*-$Pt(NH_3)_4(OH)_2^{2+}$ was determined in a like manner by observing the disappearance of the electron absorption at 578 nm. Its value was found to be $k = (4.9 \pm 0.3) \times 10^{10}$ M^{-1} s^{-1} at pH ~5.6 for concentrations of 16–50 μM. In these and other experiments described below concerning the electron reaction, the solutions contained *tert*-butyl alcohol at sufficient concentrations (0.02–0.21 M) to scavenge hydroxyl radical.[31] Results obtained on solutions saturated with N_2O indicated that the alcohol radical was itself unreactive toward $Pt(NH_3)_4(OH)_2^{2+}$. As this alcohol reacts only slowly with H atom,[32] these results also implied that hydrogen atom was unreactive toward the complex. So that this could be substantiated, solutions comprised of 0.2 M *tert*-butyl alcohol and 200 μM of complex at pH 1.9 were irradiated. Under these conditions where the electron will react preferentially with the proton to yield H atom, no significant absorption was observed in the region of 260–530 nm aside from very low levels near 260 nm, attributable in the main to the alcohol radical.[30,33] Such lack of reactivity on the part of hydrogen atom has also been reported for the analogous complex $Pt(en)_2(OH)_2^{2+}$.[20] The results presented below for the reaction of OH and $Pt(NH_3)_4^{2+}$ and that of e_{aq}^- with *trans*-$Pt(NH_3)_4(OH)_2^{2+}$ were obtained under conditions of sufficiently high concentrations of complex so that the foregoing primary processes were essentially complete before our observation period.

Reactions Associated with OH and $Pt(NH_3)_4^{2+}$. The pulse-radiolysis experiments were performed on solutions containing 100–600 μM $Pt(NH_3)_4^{2+}$ and saturated with N_2O at pH 3.3–10.2. At natural pH (ca. 5.6), there occurred a prompt development of an absorption band at about 270 nm ($\epsilon \geq 2900$ M^{-1} cm^{-1}) as shown in Figure 1. Addition of 0.2 M *tert*-butyl alcohol, an efficient scavenger of OH,[31] eliminated this development as well as subsequent ones involving both absorption and conductivity. This indicates that the phenomena reported here are derived from the nascent reaction of OH with $Pt(NH_3)_4^{2+}$. Within the time frame needed for completion of this reaction (ca. 2 μs), only very minor changes

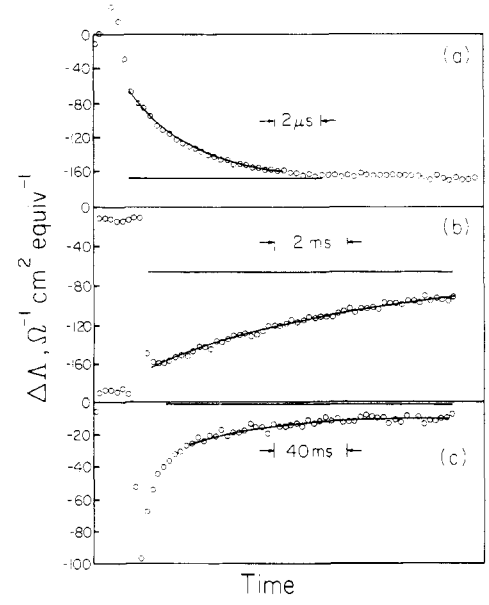

Figure 2. Equivalent conductivity changes with time, associated with the products of the reaction of OH and $Pt(NH_3)_4^{2+}$ at pH 4.2: (a) first stage, 294 μM $Pt(NH_3)_4^{2+}$; (b) second stage, 100 μM $Pt(NH_3)_4^{2+}$; (c) final stage, 100 μM $Pt(NH_3)_4^{2+}$. All solutions were saturated with N_2O.

in conductivity ($\Delta\Lambda < -50$ Ω^{-1} cm^2 $equiv^{-1}$) took place at pH 4.2 and 8.6.[35] The results are consistent with an OH addition process involving no net change in charge ($k_2 = (6.6 \pm 0.4) \times 10^9$ M^{-1} s^{-1}: vide supra).

$$OH + Pt(NH_3)_4^{2+} \xrightarrow{+H_2O} Pt(NH_3)_4(H_2O)(OH)^{2+} \quad (2)$$

The absorption peak at 270 nm is assigned to the product of this reaction. The basis for designating it as a six-coordinate species containing a bound water molecule as opposed to a five-coordinate form will be developed subsequently.

The fate of this species was strongly dependent upon the acidity or alkalinity of the media. At natural pH (ca. 5.6), the decay of the 270-nm peak obeyed a first-order rate law, with a concomitant development of two absorption bands, having peaks at about 345 and 530 nm (isosbestic point at 315 nm; Figure 1b). At longer times, the latter bands disappeared by second-order kinetics. The associated rate constant ($2k$) of $(1.0 \pm 0.2) \times 10^7$ M^{-1} s^{-1} ($\epsilon \simeq 2100$ M^{-1} cm^{-1} at 345 nm) was found to be independent of wavelength (after normalization to 345 nm), dose (10-fold), and concentration of $Pt(NH_3)_4^{2+}$ (8-fold). These features indicate that at this pH the two absorption bands are representative of a single species, A_1, whose decay involves a reaction between like species.

At a pH below 5.6, two intermediate stages were now discernible for absorption and conductivity (Figure 2), which became better resolved in time as the proton concentration was increased. The first stage was characterized by a decrease in conductivity (Figure 2a) and by enhanced rates of optical change. The resulting absorption spectrum at pH 3.3 is shown in Figure 1a. Of note is the greatly reduced absorption level at 345 nm shown at 10 μs and the indication of a new band with a possible peak below 250 nm. The level of decrease in conductivity became progressively more negative with increasing hydrogen ion concentration, attaining its largest value of -275 ± 30 Ω^{-1} cm^2 $equiv^{-1}$ at pH 3.3. Both the absorption

(35) The minor changes in conductivity are not compatible with the occurrence of a charge-transfer process yielding OH^- and $Pt(NH_3)_4^{3+}$: for such a process, substantial changes would be anticipated in acid ($\Delta\Lambda \simeq -300$ Ω^{-1} cm^2 $equiv^{-1}$) and in basic media ($\Delta\Lambda \simeq +250$ Ω^{-1} cm^2 $equiv^{-1}$).

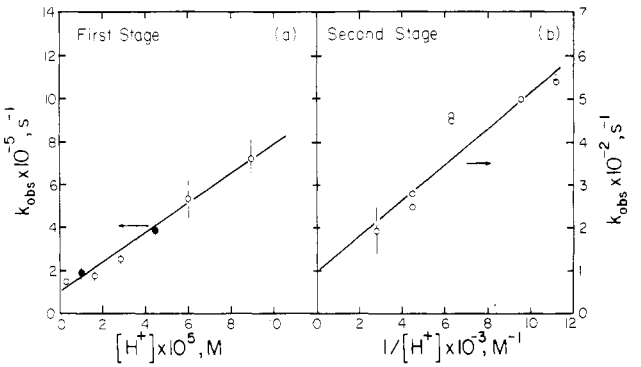

Figure 3. Effects of the proton concentration on the kinetic changes for the visible absorption bands arising from the reaction of OH and $Pt(NH_3)_4^{2+}$. (a) First stage, plot of the observed first-order rate constant for the growth in absorption vs. concentration of proton: 597 μM $Pt(NH_3)_4^{2+}$, λ = 340, 350, and 510–540 nm, intercept = (1.0 ± 0.3) × 10^5 s^{-1}, slope = (7.0 ± 0.4) × 10^9 M^{-1} s^{-1}. Filled circles represent the observed rate constants for the second stage in the absorption changes (λ = 280, 340, 530 nm) arising from the reaction of e_{aq}^- and *trans*-$Pt(NH_3)_4(OH)_2^{2+}$: 499 μM $Pt(NH_3)_4(OH)_2^{2+}$, 0.21 M *tert*-butyl alcohol. These points were not used in evaluating the plot. (b) Second stage, plot of the observed first-order rate constant vs. the reciprocal of the concentration of proton: 198–597 μM $Pt(NH_3)_4^{2+}$, λ = 340, 350, and 535–550 nm, intercept = 97 ± 42 s^{-1}, slope = (4.3 ± 0.6) × 10^{-2} M s^{-1}.

Table I. Determination of Released Ammonia and Change in Pt(II) Concentration upon Pulse Irradiation

		concn ratio[a]	
reactants	pH[b]	$[NH_3]$/[radical]	Δ[Pt(II)]/[radical][c]
OH + $Pt(NH_3)_4^{2+}$	9.5–10.4	0.39 ± 0.09 (3)	−0.28 ± 0.05 (4)[d]
	9.0	0.47	−0.07[d]
	ca. 5.6	0.16	−0.02 ± 0.02 (4)[d]
	4.4		−0.08[d]
	3.4	0.07 ± 0.05 (3)	−0.12 ± 0.03 (2)[d]
e_{aq}^- + *trans*-$Pt(NH_3)_4(OH)_2^{2+}$	9.6	1.06	
	ca. 5.6	0.44	+0.48 ± 0.07 (4)[e]
	3.4	0.49 ± 0.07 (2)	+0.39 ± 0.08 (2)[e]

[a] The symbol [radical] represents the cumulative concentration of either e_{aq}^- or OH, and the number in parentheses is the number of independent determinations. [b] The pH designated as ca. 5.6 refers to the natural pH of these solutions. [c] The algebraic sign indicates the change in platinum(II) concentration either as a net loss (−) or as formation (+). [d] Conditions: N_2O saturated; 60–250 μM $Pt(NH_3)_4^{2+}$; 20–65% reaction based upon the amount of OH reacted. The ammonia yields were not corrected for possible contributions (<13%) due to reactions of e_{aq}^- and H with starting material. [e] Conditions: He saturated; 0.2 M *tert*-butyl alcohol (one experiment at pH ca. 5.6 contained 1 M isopropyl alcohol); 100–200 μM *trans*-$Pt(NH_3)_4(OH)_2^{2+}$; 10–55% reaction based upon the amount of e_{aq}^- reacted.

and conductivity movements obeyed first-order kinetics with the same value for the observed rate constant. A plot of the observed rate constant vs. hydrogen ion concentration (Figure 3a) shows a linear dependence on $[H^+]$. The foregoing features imply a competitive situation involving the formation of species A_1 and protonation of $Pt(NH_3)_4(H_2O)(OH)^{2+}$

$$Pt(NH_3)_4(H_2O)(OH)^{2+} \rightarrow A_1 \quad (3)$$

$$H^+ + Pt(NH_3)_4(H_2O)(OH)^{2+} \rightarrow Pt(NH_3)_4(H_2O)_2^{3+} \quad (4)$$

with the product of eq 4 absorbing in the region of 250 nm. From the intercept and slope of Figure 3a, the rate constants are determined as k_3 = (1.0 ± 0.3) × 10^5 s^{-1} and k_4 = (7.0 ± 0.4) × 10^9 M^{-1} s^{-1}. Presuming that the formation of species A_1 does not reflect a change in conductivity (see below), one anticipates at pH 3.3 that the protonation process (eq 4) will be predominant and have a maximum conductivity value of

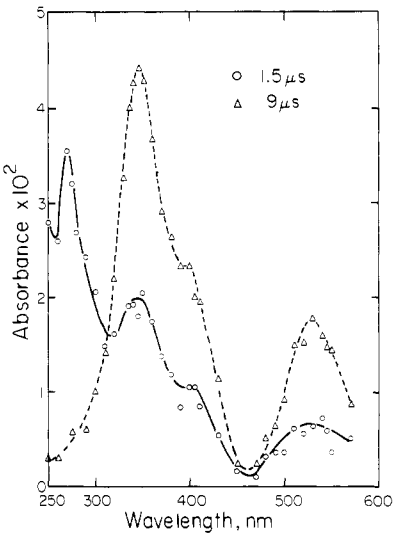

Figure 4. Absorption spectra arising from the reaction of OH and $Pt(NH_3)_4^{2+}$ in N_2O-saturated solution at pH 9.5: (○) at 1.5 μs and (△) at 9 μs with 80 μM $Pt(NH_3)_4^{2+}$ and ca. 5.4 μM OH.

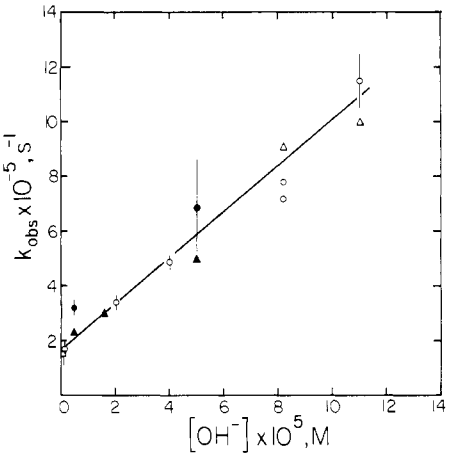

Figure 5. Effect of hydroxide ion concentration on the observed first-order rate constant arising from the reaction of OH and $Pt(NH_3)_4^{2+}$: (○) absorption change, decay at 270–290 nm, and growth at 340–530 nm, 111 or 500 μM $Pt(NH_3)_4^{2+}$; (△) decrease in conductivity, 500 μM $Pt(NH_3)_4^{2+}$. Solutions were saturated with N_2O. Intercept = (1.6 ± 0.4) × 10^5 s^{-1}; slope = (8.3 ± 0.5) × 10^9 M^{-1} s^{-1}. The filled circles and triangles represent the rate constants for absorption (λ = 270, 280, and 330–570 nm) and for conductivity associated with the second stage arising from the reaction of e_{aq}^- and *trans*-$Pt(NH_3)_4(OH)_2^{2+}$: 497 μM $Pt(NH_3)_4(OH)_2^{2+}$ and 0.21 M *tert*-butyl alcohol. This data was not used in evaluating the plot.

ca. −300 Ω^{-1} cm^2 $equiv^{-1}$ in agreement with the observed value.

The second stage was marked by a further decrease in absorption in the 260-nm region (Figure 1a) and a corresponding increase in the absorption bands at 345 and 530 nm. Both the extent and the rate of the latter became less with decreasing pH. A plot of the observed first-order rate constant describing this behavior vs. $[H^+]^{-1}$ is shown in Figure 3b.[36] Accompanying the optical changes was an increase in conductivity (Figure 2b). The prominent features at pH 3.3 were the simultaneous decay in absorption around 260 nm and an increase in conductivity to a final level of about 0. A second-order rate law was found with $2k$ = (2.8 ± 0.9) × 10^6 M^{-1} s^{-1} ($\epsilon \simeq 2350$ M^{-1} cm^{-1} at 260 nm). This was independent of dose (3-fold), and the process appears to reflect the reaction between like $Pt(NH_3)_4(H_2O)_2^{3+}$ species. At an intervening

(36) The plot shown in Figure 3b may be subject to some systematic error because the end of the second stage was not well resolved from the final stage, particularly at the lower pHs.

pH of 4.2, the second and final stages were better resolved. Here, the final stage exhibited a further increase in conductivity (Figure 2c) and a general decrease in absorption. It is particularly noteworthy that in acid media only very minor amounts of free ammonia were detected as a final product (≤16%; Table I), and thus the foregoing processes were not ones involving ammonia substitution.

In contrast, considerable free NH_3 (and loss in [Pt(II)]) was encountered at pH ≥9. Substantial alterations to the kinetic processes also transpired. The decay rate of the UV absorption band was markedly faster than at natural pH as was the growth in the visible absorption bands (Figure 4). Correspondingly, there was a decrease in conductivity, the level of which became larger in magnitude with increasing pH (the largest value of ca. $-130\ \Omega^{-1}\ cm^2\ equiv^{-1}$ was recorded at pH 10). The optical and conductivity changes were characterized by a first-order rate law. As shown in Figure 5, the observed rate constant is a linear function of hydroxide ion concentration. A notable spectral feature is the pronounced increase of about 50% in the shoulder at 400 nm (Figure 4, pH 9.55) relative to that at natural pH (Figure 1b). The enhanced presence of this shoulder in basic media indicates the formation of at least one further species, A_2, in addition to species A_1. The growth rate at 400 nm was the same as that at 345 and 530 nm. This feature in conjunction with the form of the rate law implies that the formation of A_1 via eq 3 is in competition with that for A_2.

$$OH^- + Pt(NH_3)_4(H_2O)(OH)^{2+} \rightarrow A_2 + NH_3 \quad (5)$$

From the slope in Figure 5, k_5 is associated with a value of $(8.3 \pm 0.5) \times 10^9\ M^{-1}\ s^{-1}$. The intercept yields an estimate of $k_3 = (1.6 \pm 0.4) \times 10^5\ s^{-1}$, which is in accord with that obtained from measurements performed in acidic media (Figure 3a).

Implied in eq 5 is the occurrence of a net decrease in conductivity due primarily to the consumption of hydroxide ion. The latter will however be partially mitigated by the rapid equilibrium

$$NH_3 + H_2O \rightleftharpoons NH_4^+ + OH^- \quad (6)$$

Retaining our original premise that the formation of A_1 (eq 3) does not reflect a change in charge, one then anticipates from the kinetic data, overall conductivity changes of about −25 (pH 9), −120 (pH 9.7), and $-170\ \Omega^{-1}\ cm^2\ equiv^{-1}$ (pH 10).[37] These values are in fair agreement with the observed ones of −30, −90, and $-130\ \Omega^{-1}\ cm^2\ equiv^{-1}$. The detection of free NH_3 as a final product (Table I) is supportive of this scheme although the level of NH_3 detected around pH 10 is somewhat less than that expected. This may however be an indication of analytical difficulties associated with handling ammonia containing solutions at a pH above the pK_a for NH_4^+. While A_2 appears to be an entity occurring through the loss of an ammonia ligand, its form may be similar to that of A_1, based upon the observation that the apparent molar absorption coefficients at 345 and 530 nm and their ratios (ca. 3/1) are approximately constant over the range of pH 5.6–10 whereas a significant increase occurred at 400 nm. (Support for this possibility is found below in the spectral features encountered in the electron reaction with $Pt(NH_3)_4(OH)_2^{2+}$.)

At longer times (10-ms scale), there was a general decay in the visible absorption bands accompanied by a further decrease in conductivity. The rates increased with pH, and the rate law was not in keeping with either first- or second-order behavior although the latter was a better approximation. The final level of conductivity attained (ca. −160 to $-260\ \Omega^{-1}$ $cm^2\ equiv^{-1}$ at pH 9.0) varied with dose (4-fold), being larger at smaller dose. These observations suggest a complicated mechanism, involving reactions between like and unlike species.

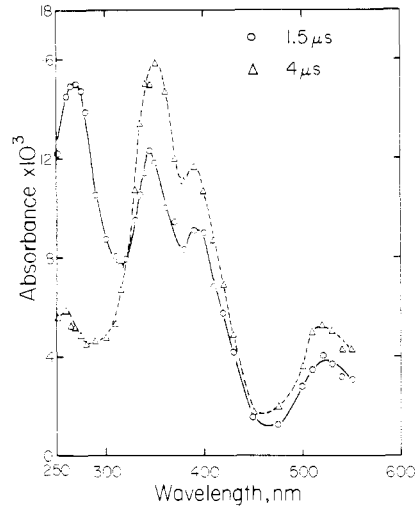

Figure 6. Absorption spectra arising from the reaction of e_{aq}^- and *trans*-$Pt(NH_3)_4(OH)_2^{2+}$ at pH 9.55: (○) at 1.5 μs and (△) at 4 μs for 192 μM $Pt(NH_3)_4(OH)_2^{2+}$, ca. 1.4 μM e_{aq}^-, and 0.20 M *tert*-butyl alcohol.

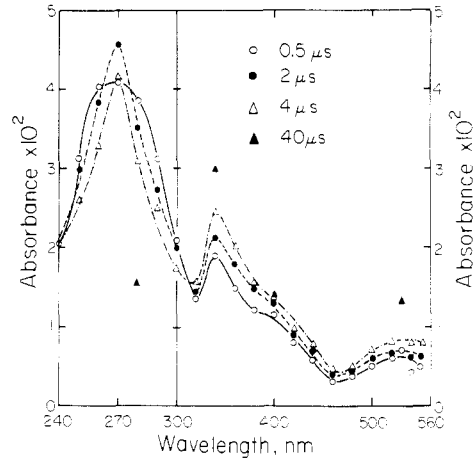

Figure 7. Absorption spectra arising from the reaction of e_{aq}^- and *trans*-$Pt(NH_3)_4(OH)_2^{2+}$ at pH 5.0: (○) at 0.5 μs, (●) at 2 μs, (△) at 4 μs, and (▲) at 40 μs for 499 μM $Pt(NH_3)_4(OH)_2^{2+}$, ca. 3.3 μM e_{aq}^-, and 0.21 M *tert*-butyl alcohol. The abscissa scale between 240 and 300 nm is expanded twofold relative to that between 300 and 560 nm.

Reactions Associated with e_{aq}^- and *trans*-$Pt(NH_3)_4(OH)_2^{2+}$. The hydrated electron reacts rapidly with $Pt(NH_3)_4(OH)_2^{2+}$, and the nascent product of this reaction is expected to be the reduced form of the complex[38]

$$e_{aq}^- + Pt(NH_3)_4(OH)_2^{2+} \rightarrow Pt(NH_3)_4(OH)_2^{+} \quad (7)$$

Under the conditions employed here (generally 0.21 M *tert*-butyl alcohol and 500 μM platinum complex at pH 3.5–9.7), this reaction with $k_7 = (4.9 \pm 0.3) \times 10^{10}\ M^{-1}\ s^{-1}$ would be complete within about 1 μs. Subsequent to this time period substantial changes in both absorption and conductivity occurred, indicating that the platinum(III) species $Pt(NH_3)_4(OH)_2^+$ underwent further reactions. As shown in Figures 6–9, the nature of these processes was strongly dependent upon the pH of the solution. That these processes were derived from the electron reaction (eq 7) was shown by their elimination

(37) The calculated conductivity changes are based on an assumed charge of 1+ for A_2.

(38) Hart, E. J.; Anbar, M. "The Hydrated Electron"; Wiley-Interscience: New York, 1970; Chapter 5.

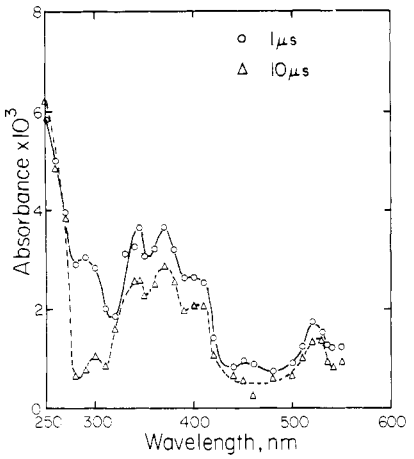

Figure 8. Absorption spectra arising from the reaction of e_{aq}^- and *trans*-$Pt(NH_3)_4(OH)_2^{2+}$ at pH 3.5: (O) at 1 μs and (Δ) at 10 μs for 188 μM $Pt(NH_3)_4(OH)_2^{2+}$, ca. 1.2 μM e_{aq}^-, and 0.20 M *tert*-butyl alcohol.

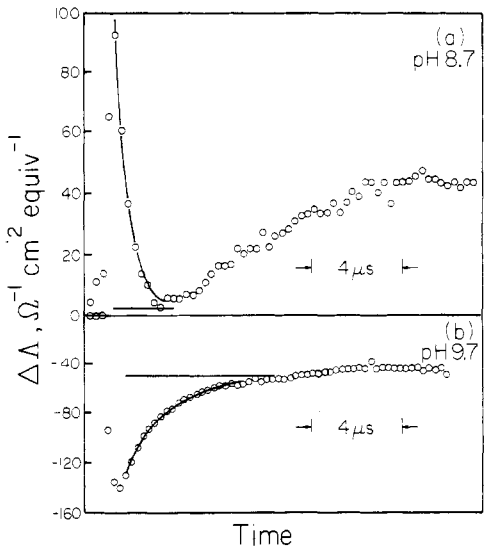

Figure 9. Equivalent conductivity changes with time, arising from the reaction of e_{aq}^- and *trans*-$Pt(NH_3)_4(OH)_2^{2+}$: (a) pH 8.7; (b) pH 9.7. Solutions contained 497 μM $Pt(NH_3)_4(OH)_2^{2+}$ and 0.21 M *tert*-butyl alcohol.

when the solutions were saturated with N_2O to scavenge e_{aq}^-.[30] Irradiation also led to the formation of platinum(II) and free ammonia as final products (Table I). Of particular note is that free ammonia was detected at all pHs with the greatest level being in basic media. The occurrence of free ammonia in the context of the electron reaction with $Pt(NH_3)_4(OH)_2^{2+}$ indicates that the transitory processes to be described below can be associated with the release of NH_3.

Considering these results in detail first for basic media, the short term changes in both absorption and conductivity took place in two stages. For the first stage, the conductivity decreased rapidly to zero at pH 8.7 with a first-order rate constant of 1.8×10^6 s^{-1} (Figure 9a). This fast decrease reflects the neutralization of the protons formed during the irradiation pulse. By this process OH^- is consumed. At pH <9 consumption is compensated by a process of similar rate giving rise to OH^-. As the pH was increased, the conductivity level attained became negative, with the largest value of −140 Ω^{-1} cm^2 $equiv^{-1}$ being measured at pH 9.7 (Figure 9b). On the same time scale, there occurred a rapid development of absorption bands with peaks at about 530, 400 (shoulder), 350, and 280 nm (Figure 6). The peak at 280 nm had an apparent molar extinction coefficient of 2800 M^{-1} cm^{-1}.

The second stage was characterized by a decay of the 280-nm band, a further growth in absorption at wavelengths above 320 nm, and a moderate increase in conductivity (Figure 6). These changes obeyed an apparent first-order rate law; however, the observed rate constants increased with increasing concentration of hydroxide ion as shown in Figure 5 (filled circles and triangles). They correspond closely in value to those (open circles and triangles in Figure 5) for the transformation of $Pt(NH_3)_4(H_2O)(OH)^{2+}$ via eq 3–5 to yield A_1 and A_2. Corroboration for the occurrence of these reactions and the presence of A_1 and A_2 is found in the comparison of the visible absorption spectra in alkaline media for the electron case (Figure 6) and for that associated with the reaction of OH and $Pt(NH_3)_4^{2+}$ (Figure 4). The positions of the peaks at ca. 350 and 530 nm are within experimental error the same as are the relative absorption coefficients ($\epsilon_{350}/\epsilon_{530} \simeq 3/1$). The salient difference resides in the 400-nm band, which we consider to be a prominent feature of A_2. In the context of the electron reaction, this feature appears as a discernible peak, whereas in the hydroxyl radical situation it is present as a shoulder of reduced intensity. These aspects imply that, in the former case, A_2 occurs in greater relative abundancy and that A_1 and A_2 exhibit similar optical qualities aside from the band at 400 nm.

In acid solutions (pH 5.0 and 4.35), there occurred initially an intensely absorbing band near 270 nm as shown in Figure 7 ($\epsilon_{270} \simeq 3500$ M^{-1} cm^{-1}). A prominent point associated with this band was its change in shape over the interval of 0.5–2 μs. A slight increase in the 270-nm peak took place over this period, whereas at higher and lower wavelengths the beginning stage of a longer term decrease in absorption occurred. This behavior suggests that the nascent electron product $Pt(NH_3)_4(OH)_2^+$ absorbs in this region and that it is rapidly being converted in part to $Pt(NH_3)_4(H_2O)(OH)^{2+}$, which also absorbs at 270 nm (Figure 1b).

At wavelengths above 315 nm, the development in absorption transpired in two stages with these being faster at lower pH. The first stage, characterized by a rapid growth in absorption with peaks at about 340 and 530 nm (shoulder at 400 nm), exhibited first-order behavior with observed rate constants of $(1.2 \pm 0.3) \times 10^6$ s^{-1} at pH 5.0 and $(3.3 \pm 0.2) \times 10^6$ s^{-1} at pH 4.35. The conductivity was marked by a decrease to −44 Ω^{-1} cm^2 $equiv^{-1}$ at pH 5.0, and at pH 4.35 an even lower value of −97 Ω^{-1} cm^2 $equiv^{-1}$. While the latter also obeyed a first-order rate law, the respective rate constants of $(6.5 \pm 0.4) \times 10^5$ and 2.8×10^6 s^{-1} were now smaller than the corresponding optical ones. The second stage was represented by a slight further decrease in conductivity: At pH 4.35, this amounted to a change from −97 to −130 Ω^{-1} cm^2 $equiv^{-1}$. Although it was not feasible to measure kinetically such a small movement, the time period for this did correspond to further alterations in the optical spectrum. As shown in Figure 7, this featured a decay in absorption at wavelengths shorter than 315 nm, an isosbestic point. Concurrently, a growth in the peaks at ca. 340 and 530 nm took place. Across the entire spectrum, the changes were describable by an apparent first-order rate law. The observed rate constants, presented as filled circles on Figure 3a, did however increase with increasing proton concentration in a manner closely paralleling that found for the first stage with respect to the transients arising from the reaction of OH and $Pt(NH_3)_4^{2+}$. This common kinetic pattern in conjunction with a common isosbestic point at 315 nm imply that in acidic media the second stage for the electron case corresponds to the first stage encountered in the context of the OH reaction, i.e., the common occurrence of $Pt(NH_3)_4(H_2O)(OH)^{2+}$ and its reactions involving eq 3 and 4.

Attempts to extend the kinetic measurements to pH conditions below 4 were complicated in part by a much reduced

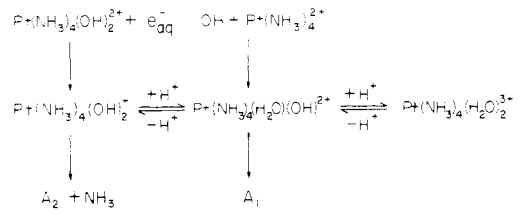

Figure 10. Proposed reaction scheme for the products arising from the reactions of e_{aq}^- and *trans*-$Pt(NH_3)_4(OH)_2^{2+}$ and of OH and $Pt(NH_3)_4^{2+}$.

level of absorption as portrayed in Figure 8. Two noteworthy features here are the occurrence of an additional peak near 370 nm, which is at a level of that for the one at 345 nm, and the greatly diminished absorption at 270 nm. The latter rapidly decayed, accompanied by increased absorption at 250 nm. Similar behavior was described above for the formation of $Pt(NH_3)_4(H_2O)_2^{3+}$ (eq 4 and Figure 1a). An additional complication to the study of these events was the subsequent and rapid decay throughout the absorption spectrum. The rates for this latter decay were nearly a 1000-fold faster than those found under similar conditions of pH and dose for the long-term behavior of the transients arising from the reaction of OH and $Pt(NH_3)_4^{2+}$. Furthermore, the kinetics did not obey either a first- or a second-order rate law. The first half-life for the decay was independent of the concentrations of platinum(IV) complex (2-fold) and of *tert*-butyl alcohol (5-fold), indicating that the starting materials were not the source of enhanced reactivity. Substitution of isopropyl alcohol for *tert*-butyl alcohol did however result in a 2–3-fold increase in the rate of disappearance of the platinum(III) transients. This suggests the involvement of reactions between the platinum(III) species and the alcohol radicals, a situation analogous to that reported in the case of platinum(III)–ethylenediamine complex ions.[20]

Discussion

The foregoing absorption and conductivity results indicate that the reactions of e_{aq}^- and $Pt(NH_3)_4(OH)_2^{2+}$ and of OH and $Pt(NH_3)_4^{2+}$ represent different entry points into a common reaction scheme. This mechanistic scheme as given in Figure 10 encompasses five platinum(III) intermediates, identified as A_1, A_2, $Pt(NH_3)_4(H_2O)_2^{3+}$, $Pt(NH_3)_4(H_2O)(OH)^{2+}$, and $Pt(NH_3)_4(OH)_2^+$. In a given circumstance, the distribution of these species depends upon the point of entry and the pH as the latter three intermediate comprise conjugate acid–base pairs. The proposed mechanism parallels that reported for the case of platinum(III)–ethylenediamine complex ions.[20] For that case, $Pt(en)_2(H_2O)(OH)^{2+}$ was identified as the nascent product of the OH addition to $Pt(en)_2^{2+}$, and this intermediate exhibits an intense absorption peak at 270 nm ($\epsilon > 4500$ M^{-1} cm^{-1}). In acidic media (pH <5), $Pt(en)_2(H_2O)(OH)^{2+}$ undergoes protonation to yield $Pt(en)_2(H_2O)_2^{3+}$ ($pK_a = 6.8$).[4,20,39] The absorption at 250 nm in acid was taken as being indicative of this transient. No direct evidence for $Pt(en)_2(OH)_2^+$ was found; however, this is the expected product from the reaction of e_{aq}^- and $Pt(en)_2(OH)_2^{2+}$.[38] Instead the initially observed product was a species having spectral features similar to those found here for A_1 and A_2. The present kinetic results as well as those for the ethylenediamine complexes show that these species arise at a secondary level. The primary products of the electron and OH reactions, observed both here and in earlier studies,[4,20,22] appear to be represented by the strong absorption bands found at short times in the region of 250–300 nm. This is partly exemplified by the results obtained at pH 9.55 for the electron reaction with $Pt(NH_3)_4(OH)_2^{2+}$ where initially a band having a peak at 280 nm is a prominent feature of the spectrum (Figure 6). The subsequent decay of this band is concomitant with an increase in absorption at longer wavelengths. This situation is further illustrated by the initial optical spectrum found at pH ca. 5.6 for the reaction of OH and $Pt(NH_3)_4^{2+}$ (Figure 1b).

For this reaction, the conductivity data is consistent with a process involving OH addition to the metal center to yield $Pt(NH_3)_4(H_2O)(OH)^{2+}$ (eq 2). The major, initial spectral feature here is an absorption band with a peak near 270 nm ($\epsilon \geq 2900$ M^{-1} cm^{-1}), whose decay is associated with the development of bands in the visible region. The location of the peak and the magnitude of the apparent absorption coefficient are close to that for $Pt(en)_2(H_2O)(OH)^{2+}$ (peak at 270 nm, $\epsilon > 4500$ M^{-1} cm^{-1}).[20] There are, however, indications that $Pt(NH_3)_4(OH)_2^+$ also absorbs in this region. Our kinetic analysis (see below) implies that the pK_a of $Pt(NH_3)_4(H_2O)(OH)^{2+}$ is near 9.8. For the reaction of e_{aq}^- and $Pt(NH_3)_4(OH)_2^{2+}$, where $Pt(NH_3)_4(OH)_2^+$ is the anticipated product, the UV band has a peak at 280 nm at pHs near 9.8. At pH 5.0, this band changes in shape over the period of 0.5–2 μs (Figure 7), with the peak now being at 270 nm. This alteration indicates contributions to this band from more than one species. Near the end of this time period, the level of conductivity (~44 Ω^{-1} cm^2 $equiv^{-1}$) can be accounted in part by the protonation of $Pt(NH_3)_4(OH)_2^+$ to give $Pt(NH_3)_4(H_2O)(OH)^{2+}$. In the *absence* of such protonation, the proton generated by the radiolytic decomposition of water (eq 1) would lead to a substantial increase in conductivity as opposed to the recorded decrease. The intensities (and locations) of the UV bands are comensurate with the transitions being of a charge-transfer character. Low-temperature ESR measurements on related Pt(III) complexes suggest that the transients encountered here are probably low-spin d^7 systems.[40] The optical electronegativities of H_2O and NH_3 are somewhat higher than that for OH^-.[41,42] It is thus reasonable to assume that these UV bands represent charge-transfer transitions of the type OH → Pt and as such would be consistent with $Pt(NH_3)_4(H_2O)(OH)^{2+}$ and $Pt(NH_3)_4(OH)_2^+$, having similar wavelength maxima for their absorption bands. This line of approach is also supportive of our assignment of the absorption near 250 nm, observed in acidic media (Figures 7b and 8), as being due to $Pt(NH_3)_4(H_2O)_2^{3+}$. As the ligands in this complex have higher optical electronegativities than that for OH^-, their corresponding charge-transfer transitions are anticipated to lie at shorter wavelengths than that for OH → Pt.

One route for the formation of the species A_1 is via the reaction of OH and $Pt(NH_3)_4^{2+}$ (eq 2), followed by eq 3. At a pH of about 5.6, only minor amounts of free ammonia were detected (and even lesser amounts at lower pH). Under this condition, A_1 appears as a major product. Consequently, it seems likely that in its formation retention of the ammonia ligands occurs. Its optical properties are however considerably different from that of its precursor, $Pt(NH_3)_4(H_2O)(OH)^{2+}$, suggesting a difference in structure between these species. The latter may be of a distorted octahedral type in view of its composition and probable low-spin d^7 character (see also ref 20). Optically A_1 appears to possess two bands of moderate

(39) The species designated as $Pt(en)_2(H_2O)(OH)^{2+}$ and $Pt(en)_2(H_2O)_2^{3+}$ were given in our earlier paper[20] as $Pt(en)_2(OH)^{2+}$ and $Pt(en)_2(H_2O)^{3+}$, respectively, upon the basis of the compositions as deduced from the kinetic results. However, other evidence was cited for their being six-coordinate species as shown here. The results of the present study are supportive of this formulation.

(40) (a) Amano, C.; Fujiwara, S. *Bull. Chem. Soc. Jpn.* **1977**, *50*, 1437. (b) Krigas, T.; Rogers, M. T. *J. Chem. Phys.* **1971**, *55*, 3035. (c) Shagisultanova, G. A.; Karaban, A. A.; Poznyak, A. L. *Khim. Vys. Energ.* **1971**, *5*, 368.
(41) Jørgensen, C. K. *Prog. Inorg. Chem.* **1970**, *12*, 101.
(42) Harzion, Z.; Navon, G. *Inorg. Chem.* **1980**, *19*, 2236.

intensity with peaks near 345 and 530 nm ($\epsilon_{345}/\epsilon_{530} \simeq 3/1$). These properties closely resemble those found for $Pt(en)(en-H)^{2+}$, where en-H designates an ethylenediamine ligand from which a proton has been removed from one of the nitrogen sites. The structure of this species has been suggested to be of a limiting square-planar form. This complex ion exhibits peaks at 340 and 480 nm ($\epsilon_{340}/\epsilon_{480} = 1.9/1$) and is formed by the elimination of water from $Pt(en)_2(H_2O)(OH)^{2+}$.[20] We would thus propose that A_1 is of the type $Pt(NH_3)_3(NH_2)^{2+}$ and that eq 3 reflects a water elimination process. As such, this reaction would not lead to a change in conductivity, in keeping with our earlier supposition.

In acidic solutions, this reaction would then be in competition with that of eq 4, one leading to the formation of $Pt(NH_3)_4(H_2O)_2^{3+}$ and accounting for the observed decrease in conductivity. This competition represents the first of two stages for the formation of A_1. Following the analysis previously developed for the Pt(III)–ethylenediamine case,[4,20] the observed rate constant for this stage, k_{obsd}, will be given by $k_3 + k_4[H^+]$. As shown in Figure 3a, k_{obsd} is linearly dependent upon proton concentration, and the values of $k_3 = (1.0 \pm 0.3) \times 10^5\ s^{-1}$ and of $k_4 = (7.0 \pm 0.4) \times 10^9\ M^{-1}\ s^{-1}$ were calculated from this data (see above). The second stage, representing a further growth in A_1, involves the reverse process of eq 4

$$Pt(NH_3)_4(H_2O)_2^{3+} \rightarrow Pt(NH_3)_4(H_2O)(OH)^{2+} + H^+ \quad (8)$$

followed by that of eq 3. This sequence however is disturbed by an additional mode of disappearance for the diaquo species. The results obtained at pH 3.3 suggest that this latter reaction may be between like species. We have however approximated this for analytical purposes by a first-order process: The small value of the intercept in Figure 3b that pertains to this reaction indicates the adequacy of this procedure. The expected dependency of k_{obsd} for the second stage on the inverse concentration of proton is realized in Figure 3b. The slope of the plot provides a measure of the ratio, k_8k_3/k_4. The value of k_8 is calculated to be $(3 \pm 1) \times 10^3\ s^{-1}$ and in conjunction with that for k_4 gives a pK_a for $Pt(NH_3)_4(H_2O)_2^{3+}$ of about 6.4, which is comparable to that of 6.8 determined for $Pt(en)_2(H_2O)_2^{3+}$.[4]

Within the framework of the proposed mechanism given in Figure 10, the reaction of e_{aq}^- and $Pt(NH_3)_4(OH)_2^{2+}$ will lead in basic media to a situation analogous to that described above, i.e., to one involving two stages of development following the electron reaction. Under our conditions, this latter process was essentially complete within a time period shorter than that of our experimental observations. At pH >6.4, formation of $Pt(NH_3)_4(H_2O)_2^{3+}$ will not occur, and the mechanistic steps will now be comprised of eq 3, 6, and 9–11.

$$Pt(NH_3)_4(OH)_2^+ \rightarrow A_2 + NH_3 \quad (9)$$

$$Pt(NH_3)_4(OH)_2^+ + H_2O \rightarrow Pt(NH_3)_4(H_2O)(OH)^{2+} + OH^- \quad (10)$$

$$Pt(NH_3)_4(H_2O)(OH)^{2+} + OH^- \rightarrow Pt(NH_3)_4(OH)_2^+ + H_2O \quad (11)$$

The assignment of eq 9 as being associated with the formation of A_2 and release of NH_3 rests with the following observations. Substantial amounts of free ammonia were detected in the case of the electron reaction, implying that the formation of ammonia originates early on in the sequence of events. The level of ammonia was largest in basic solution but it was also significant in acidic media (Table I). In contrast, only minor amounts of ammonia were found under acidic conditions for the reaction of OH and $Pt(NH_3)_4^{2+}$. In the presence of base, the level of NH_3 was now considerably higher, and within the proposed scheme is accountable through the sequence of eq 9 and 11. The absorption encountered near 400 nm and attributed primarily to A_2 is a prominent spectral point at all pHs in the case of the electron reaction (Figures 6–8). It is much less so in the context of the OH reaction with $Pt(NH_3)_4^{2+}$, and here its presence appears greatest at pH 9.5 (Figure 4).

The foregoing scheme is consistent with the two stages found in basic solutions and detected by both absorption and conductivity means. The stages were however not well separated in time, and thus the evaluation of the individual rate constants is problematical. Some reasonable estimates can be made as follows. At pH 8.7, the first stage was associated with a rapid decrease in conductivity (Figure 9a). The observed rate constant of $1.8 \times 10^6\ s^{-1}$ can be taken as an approximation of $k_9 + k_{10}$. During this stage, about 75% of the development in absorption at 340 and 400 nm transpired, and this will be controlled primarily by the ratio $k_9/(k_9 + k_{10})$. These features suggest that k_9 and k_{10} are near 1.3×10^6 and $5 \times 10^5\ s^{-1}$, respectively.[43] The observed rate constants for the second stage correspond closely to those measured in base for the reactions of $Pt(NH_3)_4(H_2O)(OH)^{2+}$ (eq 3 and 5; Figure 5). The latter were determined in the context of the OH reaction with $Pt(NH_3)_4^{2+}$, i.e., a situation in which the approach toward an equilibrium is the reverse point of view with regard to the electron reaction. Here the observed rate constants, k_{obsd}, increased in a linear fashion with hydroxide ion concentration (Figure 5). This trend and that of $k_9 > k_{10}$ and k_{obsd} suggest, that in this circumstance eq 11 may represent the rate-determining step. The value of $(8.3 \pm 0.5) \times 10^9\ M^{-1}\ s^{-1}$ for the slope of the line in Figure 5 would then be a measure of k_{11}. From this value and that for k_{10}, the pK_a of $Pt(NH_3)_4(H_2O)(OH)^{2+}$ is estimated to be 9.8. This is 3.4 units larger than the pK_a for $Pt(NH_3)_4(H_2O)_2^{3+}$. This difference seems justifiable on the ground that the second pK_a values for Pt(II) and Pt(IV) complexes containing aquo and amine ligands are typically 2–3.5 units higher than those for the first pK_a.[44]

The proposed mechanism of Figure 10 provides a consistent framework to interpret the results of this study, and it both parallels and extends the mechanism proposed earlier for the platinum(III)–ethylenediamine complex ions.[20] With regard to the species designated as A_2, it may nevertheless be an oversimplification. Spectral features, notably the peak at 370 nm shown in Figure 8, and the magnitudes of the conductivity changes encountered at the secondary level in the electron experiments suggest the possibility that A_2 could be representative of several species such as $Pt(NH_3)_3(OH)^{2+}$ and $Pt(NH_3)_2(NH_2)(OH)^+$, complexes similar in form to A_1, which is proposed to be $Pt(NH_3)_3(NH_2)^{2+}$. This resemblance would be in keeping with the apparent similarities of their spectral properties but would suggest the possible presence of addition acid–base processes. Further documentation of this is difficult to provide because the occurrence of A_2 is greatest in the case of the reaction of e_{aq}^-, and it is in this circumstance that the results point to subsequent and rapid reactions of the Pt(III) transients with the alcohol radicals. The latter processes also appear to be of consequence to the final changes in Pt(II) concentrations. The ratios of $\Delta[Pt(II)]/[radical]$, given in Table I, vary with the presence or absence of alcohol and pH. The disappearance of A_1 at near neutral pH obeyed a second-order rate law in the case of the OH reaction. If this type of behavior was representative of disproportionation of Pt(III) to yield Pt(II) and Pt(IV) products, then the ratio of $\Delta[Pt(II)]/[OH]$ should be ca. 0.5/1. The observed ratio was, however, 0.02/1. The conclusion is that the situation is more

(43) Simulation of the conductivity results shown in Figure 9 by numerical integration of the differential equations for reactions 3, 9, 10, and 11 and that for H^+ with OH^- suggest a somewhat lower value of $7 \times 10^5\ s^{-1}$ for k_9.

(44) Basolo, F.; Pearson, R. G. "Mechanisms of Inorganic Reactions", 2nd ed.; Wiley: New York, 1967; pp 32, 33.

complicated than one involving disproportionation: One possibility may involve the oxidation of water. In the presence of alcohol, the ratios of $\Delta[Pt(II)]/[e_{aq}^-]$ were near a value of 0.5/1. However, the kinetic evidence for the reactions of A_1 and A_2 with alcohol radical clearly indicates that the formation of Pt(II) resides not in disproportionation between Pt(III) species but rather in different processes.

Acknowledgment. We wish to thank the Natural Sciences and Engineering Research Council of Canada for financial support and the University of Saskatchewan for a scholarship (for H.M.K.). W.L.W. wishes to express his gratitude to the Hahn-Meitner-Institut and to the University of Saskatchewan for assistance and for the opportunity to spend periods of study at the former Institution.

Registry No. $Pt(NH_3)_4(H_2O)(OH)^{2+}$, 80243-23-8; $Pt(NH_3)_4(OH)_2^{+}$, 80243-24-9; $Pt(NH_3)_4(H_2O)_2^{3+}$, 80243-25-0; $[Pt(NH_3)_4](ClO_4)_2$, 21285-67-6; *trans*-$[Pt(NH_3)_4(OH)_2](ClO_4)_2$, 80243-26-1.

Contribution from Chemistry Department A, Technical University of Denmark, DK-2800 Lyngby, Denmark, and from Chemical Department I, H. C. Ørsted Institute, University of Copenhagen, DK-2100 Copenhagen, Denmark

Lower Oxidation States of Sulfur. 2. Spectrophotometric, Potentiometric, and ESR Study of the Sulfur-Chlorine System in Molten NaCl-$AlCl_3$ (37:63 mol %) at 150 °C

RASMUS FEHRMANN,*[1a] NIELS J. BJERRUM,*[1a] and ERIK PEDERSEN[1b]

Received January 26, 1981

Three different cationic species have been produced either by anodic oxidation or by reaction between chlorine and elemental sulfur in a NaCl-$AlCl_3$ (37:63 mol %) melt at 150 °C. Two of the species found have been identified as the radicals S_4^+ and S_8^+. No ESR signals were found for the third species, and its oxidation state is most likely $+^1/_6$, indicating that the formula may be S_{12}^{2+}. The optical spectra of the three species were calculated from measured spectra.

Introduction

In a previously published paper[2] it was shown that by anodic oxidation of sulfur it was possible to form four different cationic species in an acidic NaCl-$AlCl_3$ (37:63 mol %) melt at 150 °C. The oxidation states for the four species were found to be +4, +2, and, most likely, +1 and $+^1/_2$ corresponding to the formation of S(IV), S(II), and, possibly, S_2^{2+} and S_4^{2+}. The present investigation concerns the less oxidized forms of sulfur produced in this melt. It will be shown that two cationic radicals, S_4^+ and S_8^+, exist in the melt besides elemental sulfur and a diamagnetic species, which most likely can be formulated as S_{12}^{2+}. The latter species is analogous to the selenium species Se_{12}^{2+}, which together with Se_4^{2+}, Se_8^{2+}, and Se_{16}^{2+} was identified (with good probability) in the NaCl-$AlCl_3$ (37:63 mol %) melt.[3,4] Sulfur species with formal oxidation states $+^1/_4$ and $+^1/_8$ have previously[5] been proposed to exist in NaCl-$AlCl_3$ (37:63 mol %). This investigation did not, however, include a quantitative treatment of the spectral data because of the rather great uncertainty in the spectra. The present spectrophotometric investigation was performed with a much better signal to noise ratio of the recorded spectra and is based on a greater number of spectra.

On the basis of electrochemical investigations[6] of elemental sulfur in the NaCl-$AlCl_3$ (37:63 mol %) melt, the existence of the species S_8^+ and S_8^{2+} has recently been proposed. It should, however, be noted that intermediate species produced on an electrode surface may not be those present at equilibrium. Attempts to isolate compounds containing low oxidation states of sulfur from the system $(S_2Cl_2 + 2AlCl_3) + S_8$ (with up to 87 mol % sulfur) by cooling the wine-red liquid mixture from 150 °C failed (only elemental sulfur was recovered).[7] This melt was neutral in the sense of chlorobasicity compared to the more acidic melt used in the present work. This fact might explain why no blue color was observed since low oxidation states usually are stable only in acidic media.

The nature of the brown, green, blue, and yellow solutions of sulfur in oleum has been the subject of much controversy since they were first reported in 1804.[8] Much later two paramagnetic species were proposed to exist in these solutions.[9] From ESR measurements it was found that one had a g value around 2.016 and the other a g value around 2.026.

Several authors have investigated these two radicals (called R_1 and R_2, respectively) by ESR spectroscopy on oleum solutions of sulfur and sulfur enriched with ^{33}S. There has been especially much discussion about the formula for R_1 (in oleum or fluorosulfuric acid), which has been proposed to be S_2^+,[10] S_4^+,[11-15] S_5^+,[16,17] S_7^+,[16] or S_8^+.[18] R_2 has been much less investigated, and only a few formulas for R_2 such as S_n^+,[14] (open chain radical) or S_8^+,[13] have been proposed. The diamagnetic species S_4^{2+}, S_8^{2+}, and S_{16}^{2+} (see footnote 31) have been isolated and characterized[12,19] in crystals with SO_3F^-, AsF_6^-, SbF_6^-, and $Sb_2F_{11}^-$ as anions. These sulfur species have also been proposed[13,20] to exist in oleum solutions, and the equilibria $S_8^{2+} \rightleftarrows 2S_4^+$ and $S_{16}^{2+} \rightleftarrows 2S_8^+$ have been suggested to account for the observed increase in paramagnetism with increasing temperature in oleum solutions[13,14] and in fluorosulfuric acid.[11] The contradictory conclusions of the different

(1) (a) Technical University of Denmark. (b) University of Copenhagen.
(2) Fehrmann, R.; Bjerrum, N. J.; Poulsen, F. W. *Inorg. Chem.* **1978**, *17*, 1195.
(3) Fehrmann, R.; Bjerrum, N. J.; Andreasen, H. A. *Inorg. Chem.* **1975**, *14*, 2259.
(4) Fehrmann, R.; Bjerrum, N. J. *Inorg. Chem.* **1977**, *16*, 2089.
(5) Bjerrum, N. J. "Characterization of Solutes in Non-Aqueous Solvents"; Mamantov, G., Ed.; Plenum Press: New York, 1978; pp 251-271.
(6) Marassi, R.; Mamantov, G.; Matsunaga, M.; Springer, S. E.; Wiaux, J. P. *J. Electrochem. Soc.* **1979**, *126*, 231.
(7) Corbett, J. D. *Prog. Inorg. Chem.* **1976**, *21*, 129.
(8) Bucholz, C. F. *Gehlen's Neues J. Chem.* **1804**, *3*, 7.
(9) Gardner, D. M.; Fraenkel, G. K. *J. Am. Chem. Soc.* **1956**, *78*, 6411.
(10) McNeil, D. A. C.; Murray, M.; Symons, M. C. R. *J. Chem. Soc.* **1967**, 1019.
(11) Gillespie, R. J.; Passmore, J. *J. Chem. Soc. D* **1969**, 1333.
(12) Gillespie, R. J.; Passmore, J.; Ummat, P. K.; Vaidya, O. C. *Inorg. Chem.* **1971**, *10*, 1327.
(13) Gillespie, R. J.; Ummat, P. K. *Inorg. Chem.* **1972**, *11*, 1674.
(14) Giggenbach, W. F. *J. Chem. Soc. D* **1970**, 852.
(15) Beaudet, R. A.; Stephens, P. J. *J. Chem. Soc. D* **1971**, 1083.
(16) Symons, M. C. R.; Wilkinson, J. G. *Nature (London)* **1972**, *236*, 126.
(17) Low, S. H.; Beaudet, R. A. *J. Am. Chem. Soc.* **1976**, *98*, 3849.
(18) Stillings, M.; Symons, M. C. R.; Wilkinson, J. G. *J. Chem. Soc. D* **1971**, 372; *J. Chem. Soc. A* **1971**, 3201.
(19) Davies, C. G.; Gillespie, R. J.; Park, J. J.; Passmore, J. *Inorg. Chem.* **1971**, *10*, 2781.
(20) Stephens, P. J. *J. Chem. Soc. D* **1969**, 1496.

0020-1669/82/1321-1497$01.25/0